Title
FOCUSING IN LINEAR ION ACCELERATORS

Authors
Smith, Lloyd.
Gluckstern, Robert L.

Publication Date
1954-11-24

UNIVERSITY OF CALIFORNIA

Radiation Laboratory

BERKELEY, CALIFORNIA

DISCLAIMER

UCRL-2795
Unclassified Physics

UNIVERSITY OF CALIFORNIA
Radiation Laboratory
Berkeley, California

Contract No. W-7405-eng-48

FOCUSING IN LINEAR ION ACCELERATORS

Lloyd Smith and Robert L. Gluckstern

November 24, 1954

Printed for the U. S. Atomic Energy Commission

FOCUSING IN LINEAR ION ACCELERATORS*

Lloyd Smith

Radiation Laboratory, Department of Physics
University of California, Berkeley, California

and

Robert L. Gluckstern

Yale University, New Haven, Connecticut

November 24, 1954

ABSTRACT

The results of the investigation of three methods of obtaining transverse stability in linear accelerators for ions are presented and discussed. For electric or magnetic quadrupole focusing the range of stable operation, oscillation amplitudes, and the effect of perturbing errors are treated. For grid focusing, the operation of an actual grid is analyzed from measurements of the field distribution. Finally, the formulas applicable to focusing by axial magnetic lenses are presented.

---

*This work was performed at the Radiation Laboratory, University of California, under the auspices of the U. S. Atomic Energy Commission.

FOCUSING IN LINEAR ION ACCELERATORS*

Lloyd Smith
Radiation Laboratory, Department of Physics
University of California, Berkeley, California
and
Robert L. Gluckstern
Yale University, New Haven, Connecticut

November 24, 1954

I. INTRODUCTION

The linear accelerator suffers from the inherent difficulty that phase-stable operation necessarily gives rise to radial electric forces which are defocusing.[1] This unfortunate fact is essentially a consequence of Earnshaw's theorem applied in the rest system of the particle; if the particle rides at a potential minimum in the longitudinal direction, it cannot be at a minimum in the transverse plane. In an electron accelerator relativistic effects decrease the seriousness of the defocusing action to the extent that additional focusing is not essential. However, even a moderately short ion accelerator must be provided with some transverse focusing in order to obtain a reasonable output current.

To make matters worse, the physical layout of a linear accelerator is determined primarily by the rf requirements, and the focusing system must conform. In the Alvarez-type accelerator, for example, drift-tube shapes must be such that the cavity oscillates in the proper mode with a minimum power loss; any lens system must be designed to fit inside the drift-tube shells. Such restrictive requirements have played a significant role in retarding the development and application of ion linear accelerators.

There are two approaches to the focusing problem. One can either introduce auxiliary electric or magnetic devices to produce transverse forces, or exploit certain loopholes in the incompatibility theorem to use the accelerating fields themselves. In the first category, an axial magnetic field produced by a succession of solenoids is a simple example. The method is direct and

---

*This work was performed at the Radiation Laboratory, University of California, under the auspices of the U. S. Atomic Energy Commission.

[1] See, for example, E. M. McMillan, Phys. Rev. 80, 493 (1950).

effective, but in general requires too much power to energize the magnets. A second possibility, suggested recently by Blewett[2] after the work of Courant, Livingston and Snyder,[3] is to use a succession of electric or magnetic quadrupole lenses; it is this scheme which currently holds the greatest promise for higher-energy machines.

The most prominent system using only the accelerating field involves the introduction of grids or foils to cover the exit end of the accelerating gaps. This method is cheap and simple but of limited effectiveness, for the metallic insert cannot simultaneously resist physical wear, terminate lines of force, and transmit beam efficiently. In the two accelerators at Berkeley, which use grids, the optimum transmitted current is less by at least a factor of five than would be expected on the basis of phase acceptance alone. In machines with more drift-tubes the attenuation would certainly be greater.

Another way of circumventing the focusing difficulty has been suggested. If the ion bunch can be caused to ride alternately on the rising and the falling side of the voltage wave, the radial and longitudinal forces become alternately focusing and defocusing, resulting, for certain values of the parameters, in a stable motion for both, in exact analogy with the action of an alternating-gradient system.[4] Detailed analysis[5] has indicated definite disadvantages, which, while probably not insurmountable, have tended to discourage accelerator designers.

In this paper we present the results of some detailed studies of three of the focusing schemes: quadrupoles, grids, and solenoidal magnets. This work was done in connection with the design of the heavy-ion accelerators to be constructed at the University of California Radiation Laboratory and at Yale University;* accordingly the treatment is nonrelativistic throughout, and an Alvarez-type accelerator structure is assumed. The generalization to cases in which the rf cell lengths are not $\beta\lambda$, e.g. $1/2\ \beta\lambda$ or $2\beta\lambda$, requires only minor modification, which we have omitted for the sake of clarity. A brief development of the pertinent aspects of the phase motion and the defocusing action of the accelerating field is given in an appendix.

---

[2] J. P. Blewett, Phys. Rev. 88, 1197 (1952).

[3] Courant, Livingston, and Snyder, Phys. Rev. 88, 1190 (1952).

[4] J. H. Adlam, AERE-GP/M-146, Harwell, Berks. (England) (1953); M. L. Good, Phys. Rev. 92, 538 (1953).

[5] L. B. Mullett, AERE-GP/M-147, Harwell, Berks. (England) (1953).

* These accelerators will consist, in succession, of a 500 kv Cockroft-Walton, a grid-focused accelerator cavity up to 1 Mev per nucleon, a device to remove additional ion electrons, and a magnetic strong-focused accelerator cavity up to a terminal energy of 10 Mev per nucleon.

II. QUADRUPOLE LENSES

A. Radial Stability

We shall consider an accelerator consisting of a succession of drift tubes of increasing length held on the axis of a resonant cavity. The drift tubes are thin shells which contain electric or magnetic quadrupole lenses, the necessary electrical connections being made through the drift-tube supports. The lenses may all have the same orientation about the beam axis, or they may be rotated in a regular manner from one drift-tube to the next. In the latter case the formal treatment is more complicated, but the results are essentially the same, so that we shall confine ourselves to lenses of identical orientation but with a variety of polarity groupings.

The ion trajectories can be decomposed into independent motions in two mutually perpendicular transverse directions, which we shall denote by x and y, z being the direction of motion of the beam. In either plane, the ion sees a succession of focusing and defocusing forces in the lenses, force-free regions outside of the lenses, and rf radial forces which we treat as impulses at the center of the accelerating gaps.

The orbits can be traced through the various sections most easily by using a matrix formalism.[6] Considering x (or y) and $\dot{x}/\nu$ (or $\dot{y}/\nu$), where ν is the cavity frequency, as components of a vector, the effects of the quadrupole elements are described by the matrices

$$M_+ = \begin{pmatrix} \cos\theta & \frac{\sin\theta}{\theta_o} \\ -\theta_o \sin\theta & \cos\theta \end{pmatrix} \tag{1}$$

in a focusing plane and

$$M_- = \begin{pmatrix} \cosh\theta & \frac{\sinh\theta}{\theta_o} \\ \theta_o \sinh\theta & \cosh\theta \end{pmatrix} \tag{2}$$

in a defocusing plane. Here $\theta = (\omega_{sf}\, \ell_{sf}/\beta c)$ and $\theta_o = (\omega_{sf}/\nu)$, where βc is the ion velocity, ℓ_{sf} is the length of the focusing or defocusing element, and $\pm m\omega_{sf}^2$ is the effective spring constant of either the focusing or defocusing fields, i.e.

$$\omega_{sf}^2 = (eH'\beta/m) \text{ or } \omega_{sf}^2 = (eE'/m) \tag{3}$$

---

[6] See, for example, L. A. Pipes, J. Appl. Phys. 24, 902 (1953).

for a magnetic or electric quadrupole with field gradient E' or H'.

The matrix corresponding to a field-free section of length ℓ may be written as

$$M_o = \begin{pmatrix} 1 & 1-\Lambda \\ 0 & 1 \end{pmatrix} \tag{4}$$

where

$$1-\Lambda = (\ell/\beta\lambda) = (\ell\nu/\beta c), \tag{5}$$

and the matrix corresponding to the action of a gap is

$$M_g = \begin{pmatrix} 1 & 0 \\ -\Delta & 1 \end{pmatrix} \tag{6}$$

in the approximation that all the defocusing is concentrated at the gap center. Here

$$\Delta = \frac{\pi e E \lambda T \sin \phi}{mc^2 \beta}, \tag{7}$$

the net radial rf impulse per unit displacement, as derived in the appendix.

The advantage of the matrix notation is that the effect of a succession of sections is obtained by multiplying in proper order the corresponding matrices. For example, if lens polarity alternates in successive drift tubes* (known hereafter as the N = 1 grouping†) and drift spaces and rf forces are neglected, the position-velocity vector at the center of a focusing section is related to that at the center of the preceding focusing section by the equation

$$\begin{pmatrix} x^f \\ \dot{x}^f/\nu \end{pmatrix}_{n+1} = \begin{pmatrix} \cos(\theta_o/2) & \frac{\sin(\theta_o/2)}{\theta_o} \\ -\theta_o \sin(\theta_o/2) & \cos(\theta_o/2) \end{pmatrix} \begin{pmatrix} \cosh\theta_o & \frac{\sinh\theta_o}{\theta_o} \\ \theta_o \sinh\theta_o & \cosh\theta_o \end{pmatrix}$$

$$\times \begin{pmatrix} \cos(\theta_o/2) & \frac{\sin(\theta_o/2)}{\theta_o} \\ -\theta_o \sin(\theta_o/2) & \cos(\theta_o/2) \end{pmatrix} \begin{pmatrix} x^f \\ \dot{x}^f/\nu \end{pmatrix}_n \tag{8}$$

*The case N = 1 has been treated by L. C. Teng, Rev. Sci. Instr., 25, 264 (1954) in connection with the Minnesota accelerator.

†The integer N corresponds to the number of lenses between polarity alternations.

However complicated the configuration, the product matrix representing a full repeat length from the center of a polarity grouping to the next corresponding point is of the form

$$M_N = \begin{pmatrix} \cos \mu_N & \gamma_N \sin \mu_N \\ -\frac{\sin \mu_N}{\gamma_N} & \cos \mu_N \end{pmatrix}. \tag{9}$$

That is, the diagonal elements are equal and the determinant is unity, so that the matrix is characterized by two independent quantities. The subscript is used to distinguish polarity groupings.

Once μ_N and γ_N are determined, the trajectory can be propagated easily,* for

$$(M_N)^n = \begin{pmatrix} \cos n\mu_N & \gamma_N \sin n\mu_N \\ -\frac{\sin n\mu_N}{\gamma_N} & \cos n\mu_N \end{pmatrix} \tag{10}$$

Thus the condition for stability is that $\cos n\mu_N$ be bounded, or that μ_N be real.

The quantity $\cos \mu_N$ has been calculated numerically for N = 1, 2, and 3 over the range of parameters of interest for linear accelerators, but with the restriction that the lens elements and drift spaces are of equal length ($\Lambda = 1/2$). The results are presented in Figs. 1, 2, 3. It can be seen that for given Δ the required focusing fields decrease with N. However, the relative height and width of the stable region also decrease, restricting the available range of operating points. Since Δ depends on the ion phase at the accelerating gaps, phase oscillations sweep the ions over a considerable range of positive and negative values of Δ.

We believe that, at the present stage of the art of strong focusing, we are not being unduly cautious in asking that the representative point should stay inside the stable region for all ions at all times. This requirement, together with the feasibility of attaining the necessary focusing fields,

*In writing Eq. (10) as the product of identical matrices we have assumed that the parameters γ_N and μ_N are constant along the accelerator. A slow variation of these parameters leads to a modulation of the amplitude of radial oscillation discussed later.

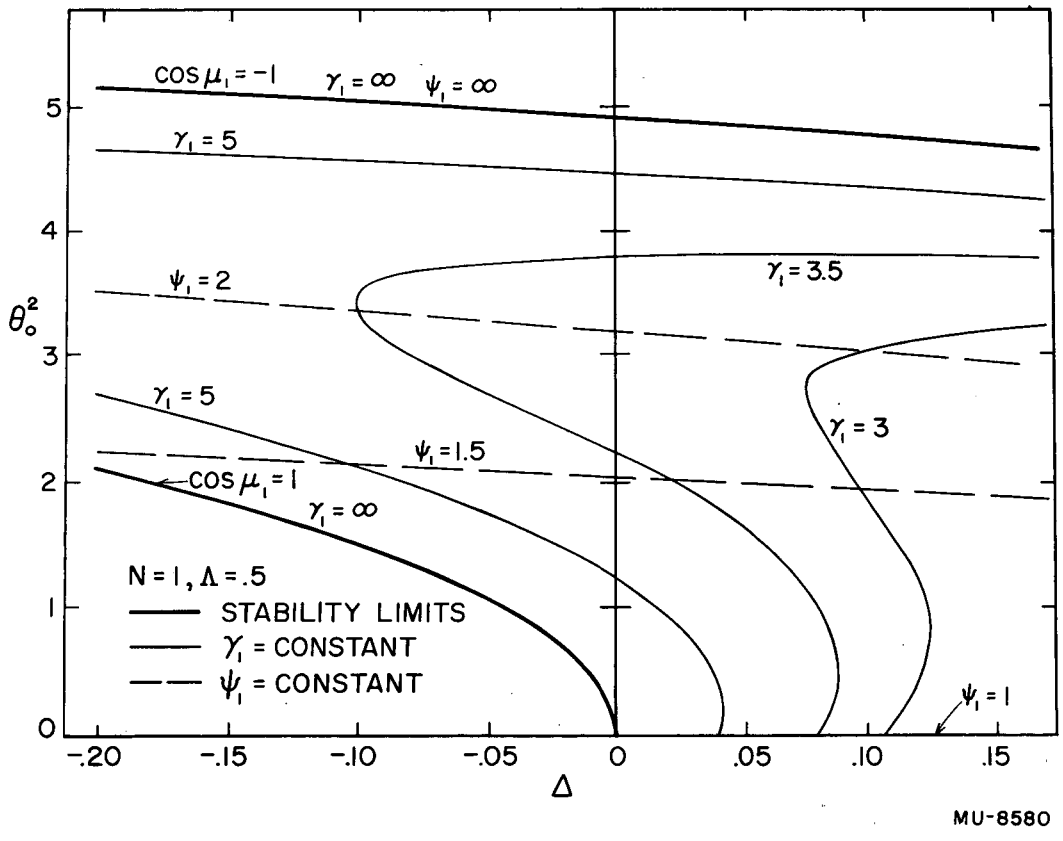
cos μ₁ = -1
γ₁ = ∞
ψ₁ = ∞
γ₁ = 5
ψ₁ = 2
γ₁ = 3.5
γ₁ = 5
γ₁ = 3
ψ₁ = 1.5
cos μ₁ = 1
γ₁ = ∞
N = 1, Λ = .5
STABILITY LIMITS
γ₁ = CONSTANT
ψ₁ = CONSTANT
ψ₁ = 1
θ₀²
Δ
0
1
2
3
4
5
-.20
-.15
-.10
-.05
0
.05
.10
.15
MU-8580

Fig. 1.

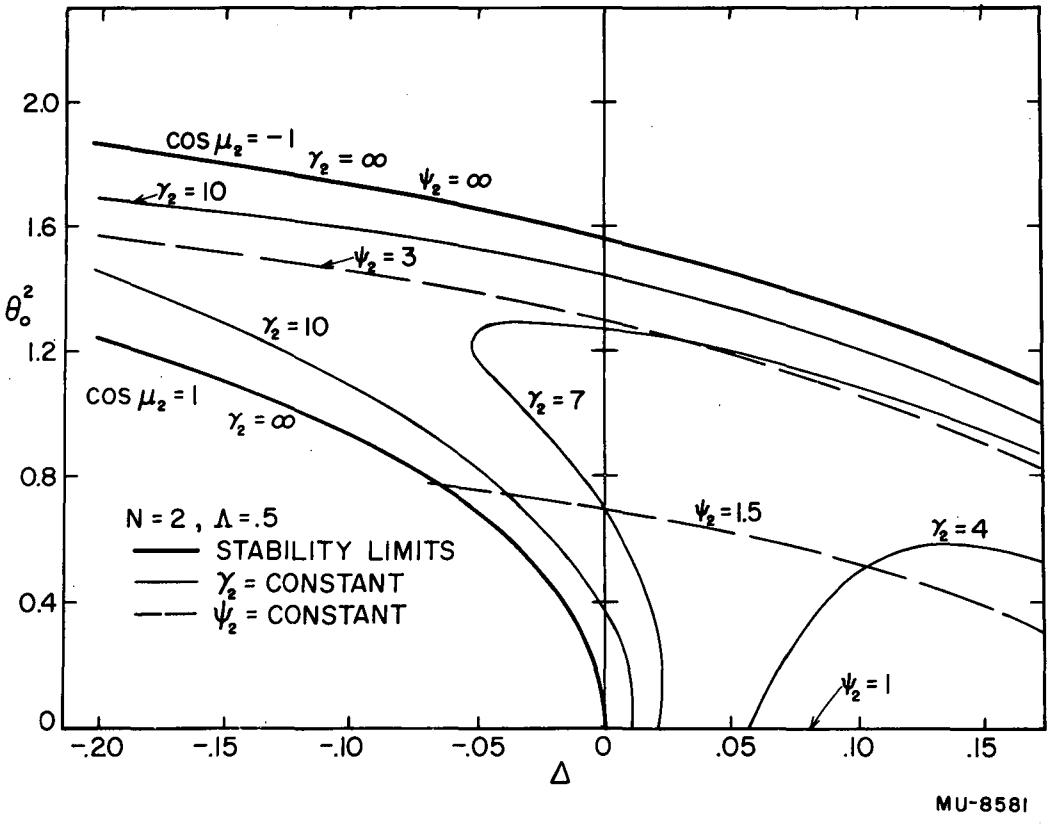
2.0
1.6
1.2
0.8
0.4
0
θ_o^2
$\cos\mu_2 = -1$
$\gamma_2 = \infty$
$\psi_2 = \infty$
$\gamma_2 = 10$
$\psi_2 = 3$
$\gamma_2 = 10$
$\cos\mu_2 = 1$
$\gamma_2 = \infty$
$\gamma_2 = 7$
$\psi_2 = 1.5$
$\gamma_2 = 4$
$\psi_2 = 1$
N = 2 , Λ = .5
STABILITY LIMITS
γ_2 = CONSTANT
ψ_2 = CONSTANT
-.20
-.15
-.10
-.05
0
.05
.10
.15
Δ
MU-8581

Fig. 2.

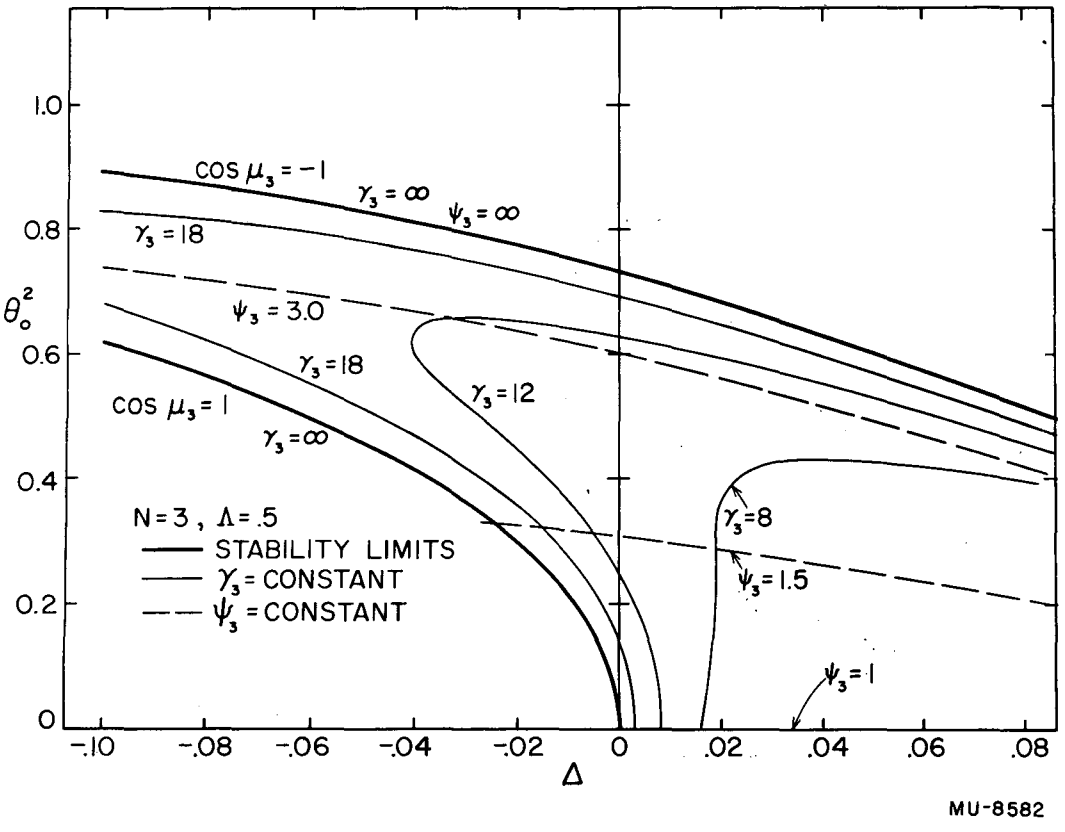
1.0
0.8
0.6
0.4
0.2
0
θ_o^2
-.10
-.08
-.06
-.04
-.02
0
.02
.04
.06
.08
Δ
cos μ_3 = -1
$\gamma_3 = \infty$
$\psi_3 = \infty$
γ_3 = 18
ψ_3 = 3.0
γ_3 = 18
γ_3 = 12
cos μ_3 = 1
$\gamma_3 = \infty$
N = 3, Λ = .5
STABILITY LIMITS
γ_3 = CONSTANT
ψ_3 = CONSTANT
γ_3 = 8
ψ_3 = 1.5
ψ_3 = 1
MU-8582

Fig. 3.

essentially determines the design parameters of a given accelerator.

For example, consider the 32-Mev proton accelerator at Berkeley. In this machine Δ ranges from - 0.08 to + 0.04 at the entrance end. The largest grouping that should be used is N = 3, with a value of $\theta_o^2 = 0.6$ for $\Lambda = 0.5$. For a 3/4-in. bore, the voltage would be ± 11 kv in the electric case, or the pole-tip field would be 850 gauss in the magnetic case.

In the heavy-ion accelerator Δ ranges from - 0.09 to + 0.05 at the beginning of the quadrupole-focused section. Electromagnets will definitely be used, allowing a choice between N = 1 and N = 2. The pole-tip fields are 7 and 4 kilogauss respectively. In the interest of saving power, it is intended to try the N = 2 configuration first, but the magnets are designed to provide the higher fields required for N = 1.

A feature of the strong-focusing system of interest in the heavy-ion accelerator is that ions with several values of e/m can be accommodated simultaneously. Larger values of e/m lead to larger values of Δ for the same electrical gradient, but the magnetic forces are stronger as well. As presently designed, the heavy-ion machine will accelerate ions with e/m = 0.27 to 0.40 of proton e/m for N = 2, and e/m = 0.27 to 0.75 for N = 1.

For quadrupole elements of arbitrary length, the limits of the stability region may be plotted with reasonable accuracy from the following general expansion of $\cos \mu_N$:

$$\cos \mu_N = \left\{1 - \left[\frac{N^2(N^2 + 2 - 2\Lambda)}{6}\right]\Lambda^2\theta_o^4 - \cdots\right\}$$

$$- \frac{4N^2}{2!}\Delta\left\{1 - \left[\frac{2+35N^2+8N^4-5\Lambda(1+8N^2)+5\Lambda^2(2+N^2)-3\Lambda^3}{360}\right]\Lambda^2\theta_o^4 + \cdots\right\}$$

$$+ \frac{8N^2(N^2-1)}{4!}\Delta^2\left\{1 + \cdots\right\} - \frac{16N^2(N^2-1)(N^2-4)}{6!}\Delta^3\left\{1 + \cdots\right\} + \cdots . \quad (11)$$

B. Oscillation Amplitudes

We shall use the following properties***** of strong-focusing systems without proof:

(1) Maximum displacement occurs at the center of a focusing group for any initial displacement and velocity.

(2) For a parallel entering beam, i.e. one in which the angular divergence is small compared to the angles introduced in the lens system, the

***** The fact that for even N the center of a polarity grouping occurs at an accelerating gap does not substantially affect the validity of these statements.

maximum displacement is smallest if the lens system begins at the center of a polarity grouping.

(3) For a divergent entering beam, i.e., one in which the diameter is small compared to the displacement produced by the lens system, the maximum displacement is smallest if the lens system begins at a transition point between polarity groups.

We shall also use the fact, which may be verified by applying Eq. (10), that the quantity

$$(X^f)^2 = (x_n^f)^2 + \gamma_N^2 \left(\frac{\dot{x}_n^f}{\nu}\right)^2 , \tag{12}$$

evaluated at the center of focusing groups, is independent of n. The existence of such an invariant is reminiscent of energy conservation in simple harmonic motion. Because of property (1) X^f can therefore be interpreted as an amplitude, for it is the maximum value of the displacement at the center of a focusing group and therefore the largest displacement attained at any time.

Since it is more likely that preaccelerated beams are parallel than divergent in the sense used above, we shall consider in detail only the case of entering in the center of a polarity group. A different starting point may be handled by first performing an appropriate number of matrix multiplications to translate starting conditions to the nearest group center.

The amplitude X^f for parallel injection in the focusing plane is

$$X^f(\dot{x}_o^f = 0) = x_o^f , \tag{13}$$

and if there is angular divergence

$$X^f(x_o^f = 0) = \gamma_N \left(\frac{\dot{x}_o^f}{\nu}\right) . \tag{14}$$

The maximum excursion in the initially defocusing yz plane requires the evaluation of the matrix connecting the center of a focusing region to the center of a defocusing region. The corresponding amplitudes may be written as

$$X^d(\dot{x}_o^d = 0) = \psi_N x_o^d , \tag{15}$$

$$X^d(x_o^d = 0) = \frac{\gamma_N}{\psi_N} \left(\frac{\dot{x}_o^d}{\nu}\right) \tag{16}$$

where ψ_N^2 is the ratio of the 22 to the 11 element of the "half matrix".

Figs. 1, 2, 3 contain lines of constant γ_N and constant ψ_N for the case $\Lambda = 1/2$ obtained from the following approximate forms:

$$\gamma_N = \frac{2N\left[1 + \left\{\begin{matrix} n^2 + 1 \\ n^2 \end{matrix} -\Lambda\right\} \frac{\Lambda\theta_o^2}{2} - \frac{\Delta}{12}\left\{\begin{matrix} 8n^2 + 1 \\ 8n^2 - 2 \end{matrix}\right\}\right]}{\sin \mu_N} \tag{17}$$

$$\psi_N = \frac{1 + \left\{\begin{matrix} n^2 + 1 \\ n^2 \end{matrix} -\Lambda\right\} \frac{\Lambda\theta_o^2}{4} - \frac{\Delta}{2} n^2}{\cos (\mu_N/2)} \,. \tag{18}$$

Where there is a choice within the brace $\left\{\ \right\}$, the upper quantity is for odd N, and the lower for even N.

It is clear from Figs. 1, 2, 3 that the boundaries of the stability region are to be avoided in any practical design. The size and divergence of the incoming beam, however, will influence the exact choice of an operating region.

As previously mentioned, a variation of the parameters γ_N or μ_N along the accelerator leads to modulation of the amplitude of the radial oscillation. Two features of this modulation are pertinent:

(1) Except for the special case mentioned below, the amplitude of radial motion (X^f in Eq. (12)) will vary as $\gamma_N^{1/2}$. Unfortunately this cannot be used to contract the beam appreciably, since one is confined by the phase oscillations to an average Δ which is negative.

(2) A resonance between the phase and radial motion occurs when the phase oscillation frequency is twice the radial oscillation frequency. The seriousness of this resonance depends on how precisely this resonance condition is maintained, and also on the total length of the accelerator, since both oscillations in question have long periods. The portion of the stability region corresponding to this resonance is quite close to the $\cos \mu_N = +1$ border and can be avoided without any difficulty.

C. Effect of Random Errors

A serious disadvantage to this focusing scheme is an extreme sensitivity to random errors in the positions and strengths of the lens elements. We shall consider the following types of imperfections:

(1) Displacement and tilt of the axis of zero field,

(2) Angular misalignment of the transverse axes,

(3) Fluctuations of lens strengths about some programmed values.

The calculation of the induced oscillations is greatly simplified, without loss of the essential features, by neglecting the normal variation of the displacement in traversing a lens, and computing the additional transverse impulse due to the imperfection. This impulse causes a certain change in amplitude; the average value of these changes is of course zero, but the mean-square induced amplitude is the sum of the mean-square contributions of the individual sections.

The transverse impulse in each case is:

$$(1) \quad (\delta \dot{x}/v) = (1/2)\, \Lambda\theta_o^{\,2}(\Delta x_i + \Delta x_f), \tag{19}$$

where Δx_i and Δx_f are the displacements of the entrance and exit ends of the lens;

$$(2) \quad (\delta \dot{x}/v) = -\, 2\Lambda\theta_o^{\,2} y\, \Delta\alpha, \quad (\delta \dot{y}/v) = 2\Lambda\theta_o^{\,2} x\, \Delta\alpha, \tag{20}$$

where $\Delta\alpha$ is the angular error in orientation of the axes;

$$(3) \quad (\delta \dot{x}/v) = \Lambda\theta_o^{\,2} x\epsilon, \tag{21}$$

where ϵ is the fractional error in field strength.

The amplitude changes due to these transverse impulses are given, for radial oscillations of moderately long wave length, by

$$\delta A^x = \gamma_N^{\,2} \frac{(\dot{x}/v)}{A^x} \Sigma\, \delta(\dot{x}/v) \,. \tag{22}$$

If one averages the square of the amplitude changes over the phases of the unperturbed radial oscillations, and considers all the perturbing errors as random, the rms amplitude change in each case introduces a factor $\gamma_N(\mathcal{N})^{1/2}$, apart from a numerical constant, for $\mathcal{N}$ quadrupole elements. Specifically, one obtains

$$\delta A^x{}_{rms} = \gamma_N \Lambda\, \theta_o^{\,2} (\mathcal{N})^{1/2} \left[\frac{\langle (\Delta x)^2 \rangle}{4} + (A^y)^2 \langle (\Delta\alpha)^2 \rangle + \frac{(A^x)^2 \langle (\epsilon)^2 \rangle}{8} \right]^{1/2} \tag{23}$$

and

$$\delta A^y{}_{rms} = \gamma_N \Lambda\, \theta_o^{\,2} (\mathcal{N})^{1/2} \left[\frac{\langle (\Delta y)^2 \rangle}{4} + (A^x)^2 \langle (\Delta\alpha)^2 \rangle + \frac{(A^y)^2 \langle (\epsilon)^2 \rangle}{8} \right]^{1/2} \tag{24}$$

where $\langle f^2 \rangle$ stands for the average square of f.

The errors all contribute to the effect in similar ways; in all cases the seriousness of the effect is determined by the quantity γ_N, which is generally large, approaching infinity at the boundaries of the stability region.

The mean-square values, if anything, underemphasize the effect, for in a machine of moderate length the deviations will most probably exceed the mean-square values at one or more points. If the drift-tube bore diameter is increased steadily to accommodate only the anticipated mean-square growth in amplitude, some loss occurs. Because the focusing voltages and pole-tip field strengths increase substantially as the bore increases, it is necessary to effect a compromise in design. Since no strong focusing accelerator exists as yet, the problem cannot be properly evaluated, but it would appear that the utmost care in construction and assembly is necessary to obtain maximum output current.

We have checked the mean-square calculations by computing exactly the orbits in the heavy-ion accelerator for several selections of random errors with the help of an IBM card programmed calculator. The 30 cases tried verified the above formulas in the mean-square sense, but three showed amplitude changes of about twice the rms value. Several runs were made with the same set of errors but with different values of the rf defocusing impulse to get an indication of the effect of phase oscillations. The resulting amplitudes were similar in magnitude, but the maximum displacements occurred at widely separated points, indicating that the transmitted beam will simply be larger in diameter and not displaced to one side.

The effect of random errors in the spacing between lenses has also been considered. It is small compared to the three effects discussed above, since no large perturbing forces are introduced by errors in the lengths of the field-free sections.

D. Fringing Fields

The principal effect of the fringing fields in either the electric or magnetic case is to make the effective length of the element longer than its physical length. Since Eq. (11) depends primarily on the combination $\Lambda\theta_o^2$, the quantity which enters into the dynamics is $\int H' dz$ or $\int E' dz$.

An effect peculiar to the magnetic strong-focusing system is the coupling that arises between the motions in the two transverse planes owing to the longitudinal component of the fringing field, in the region where the polarity of the

quadrupole element changes. It can be shown that this coupling allows a transfer of energy of transverse motion from one plane to the other. The amount depends only on the initial conditions; the rate of transfer depends on the magnitude of the coupling. Numerical values for the heavy-ion machine indicate that the increase in radial amplitude in either plane might be appreciable were it not for the fact that the coupling constant is quite small.

III. GRID FOCUSING[7]

An ion crossing an open accelerating gap while the gap voltage is increasing as required for phase stability is defocused because the outward radial field it encounters on leaving the gap is stronger than the inward field through which it passed on entering the gap. A foil or grid placed at the exit end of the gap is intended to intercept the lines of force before they begin to bend outward to end on the drift-tube surface. If the action is perfect and field penetration at the gap entrance is negligible, the net radial impulse in crossing a gap is equal to that experienced on entering the gap:

$$\Delta \dot{r} = \frac{e}{m\beta c} \int E_r \cos\left(\frac{2\pi z}{L} + \phi\right) dz \cong \frac{-e\, E_g \cos\left(\phi - \frac{\pi g}{L}\right)}{2m\beta c}\, r \qquad (25)$$

where E_g is the maximum rf gradient in the gap.

The phase at successive gaps is determined by the phase oscillations, so that the resulting radial motion is rather complicated. It is certainly stable, however, if

$$\phi \geq -\frac{\pi}{2} + \frac{\pi g}{L} \,. \qquad (26)$$

Since the maximum negative phase excursion is approximately twice the synchronous phase ϕ_s, the orbits are stable if

$$\phi_s \geq -\frac{\pi}{4} + \frac{\pi g}{2L} \,. \qquad (27)$$

---

[7] Grid focusing has been treated principally by W. K. H. Panofsky, UCRL-1216 (1951) and more recently by J. S. Bell, AERE-T/M-95, Harwell, Berks. (England) 1954.

The range of choices of g/L in an Alvarez-type accelerator is rather restricted. If the gaps are short, the gap fields become too high for a reasonable average rate of energy gain, while the transit time factor suffers if the gaps are long. The traditional choice is g/L = 1/4, so that true stability is lost at $\phi_s \sim -22.5^\circ$. Actually, complete stability is not necessary, for even if the phase motion swings beyond this limit, the rate of increase of radial momentum may be small enough to permit most of the ions to get through.

For actual grids, one cannot expect the perfect behavior described above. In order to study the performance of an actual grid, field distributions in gaps terminated by the type of grid shown in Fig. 4 were measured in a three-dimensional electrolytic tank.† This grid configuration is the one which was adopted in both Berkeley accelerators after considerable experimentation. Measurements were made for two ratios of gap length to bore radius: 1.625 and 3.25.

The quantity of interest for the radial motion is the radial impulse experienced by a particle in crossing a gap. For a constant radial displacement in a gap,

$$\Delta \dot{r} = \frac{e}{m\beta c} \int E_r(r, \theta, z) \cos\left(\frac{2\pi z}{L} + \phi\right) dz, \qquad (28)$$

where $E_r(r, \theta, z)$ is the radial electric field expressed as a function of radius, azimuth, and axial position in the gap.

Since the measurements were of potentials, it is convenient to rewrite the impulse

$$\Delta \dot{r} = \frac{eE\beta\lambda^2}{2\pi mc}\left[\cos\phi \frac{\partial S(r, \theta)}{\partial r} - \sin\phi \frac{\partial C(r, \theta)}{\partial r}\right], \qquad (29)$$

where

$$S(r, \theta) = -\int_{-\infty}^{\infty}\left[\frac{V(r, \theta, z) - V(0, \theta, z)}{\Delta V}\right] \cos\frac{2\pi z}{L}\, d\left(\frac{2\pi z}{L}\right), \qquad (30)$$

† The use of Laplace's equations for the electric field is justified if the dimensions of the region of interest are small compared to the wavelength. This is true for the gaps where $\beta << 1$.

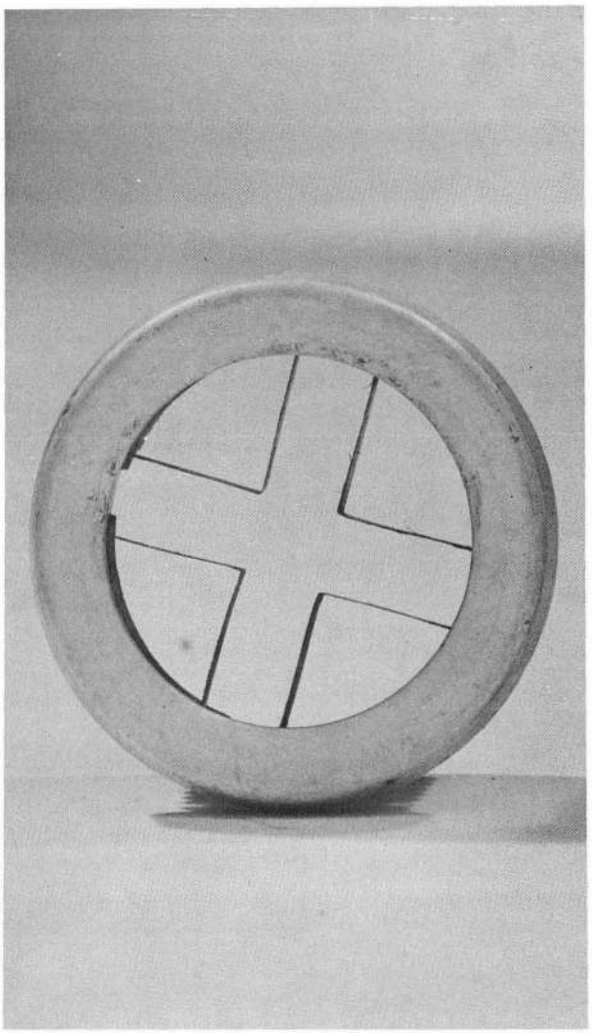

ZN-2687

Fig. 4.

$$C(r, \theta) = -\int_{-\infty}^{\infty} \left[\frac{V(r, \theta, z) - V(0, \theta, z)}{\Delta V}\right] \sin \frac{2\pi z}{L}\, d\left(\frac{2\pi z}{L}\right) . \qquad (31)$$

Here E is the average rf gradient along the accelerator (= g E_g/L) and $V(r, \theta, z)$ is the measured potential, the total difference in potential between drift-tubes being ΔV. Figures 5 and 6 contain plots of $C(r, \theta)$, and $S(r, \theta)$ as a function of r/a for g/a = 1.625, using g/L = 1/4. The results for g/a = 3.25 are quite similar and are not shown. $C(r, \theta)$ and $S(r, \theta)$ depend surprisingly little on the azimuthal angle θ; it therefore seems reasonably safe to average the radial impulse over θ, especially if the grids are oriented differently from each other.

In general the radial impulse is small enough so that the radial motion through a large number of drift tubes can be adequately described by the second-order equation

$$\ddot{r} = \nu \Delta \dot{r} = \frac{eE\beta\lambda}{2\pi m} \left[\cos \phi \frac{dS(r)}{dr} - \sin \phi \frac{dC(r)}{dr}\right] , \qquad (32)$$

where $C(r) = \left\langle C(r, \theta)\right\rangle_\theta$ and $S(r) = \left\langle S(r, \theta)\right\rangle_\theta$.

If one for the moment neglects the variation of β, ϕ, S(r), and C(r) along the machine (at a given value of r), Eq. (32) has a first integral

$$\frac{m\dot{r}^2}{2} + \mathcal{V}(r) = \epsilon , \qquad (33)$$

where

$$\mathcal{V}(r) = \frac{eE\beta\lambda}{2\pi} \left[-\cos \phi\, S(r) + \sin \phi\, C(r)\right] . \qquad (34)$$

Figures 7 and 8 show $(2\pi\mathcal{V}(r))/(eE\beta\lambda)$ for values of ϕ from -40° to $+40^\circ$, with g/a = 1.625 and 3.25 respectively. It is apparent that the radial motion is completely stable only for phases greater than $\sim -20^\circ$ for g/a = 1.625 and $\sim -30^\circ$ for g/a = 3.25. In addition there is a small pocket at r ~ 0.4a in which stable motion is possible with small radial velocity for phases as low as -30° for g/a = 1.625 and $\sim -40^\circ$ for g/a = 3.25.

The potential for a perfect grid is readily obtained from Eq. (25) as

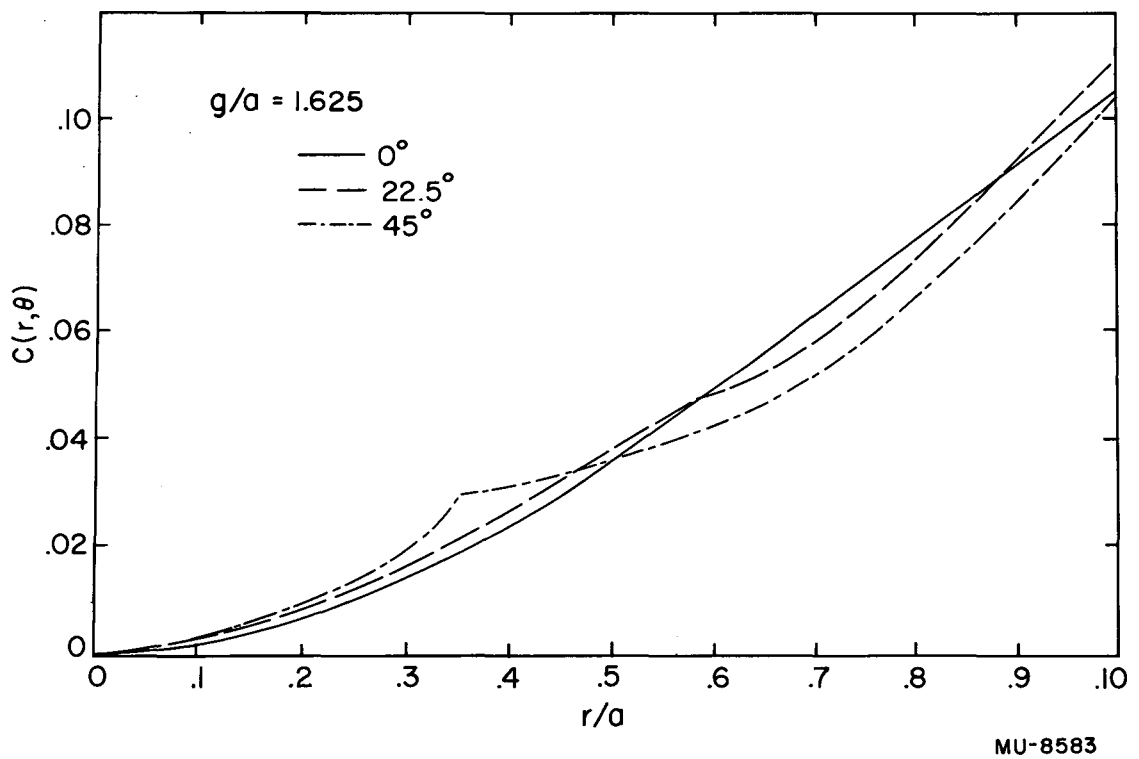

Fig. 5.

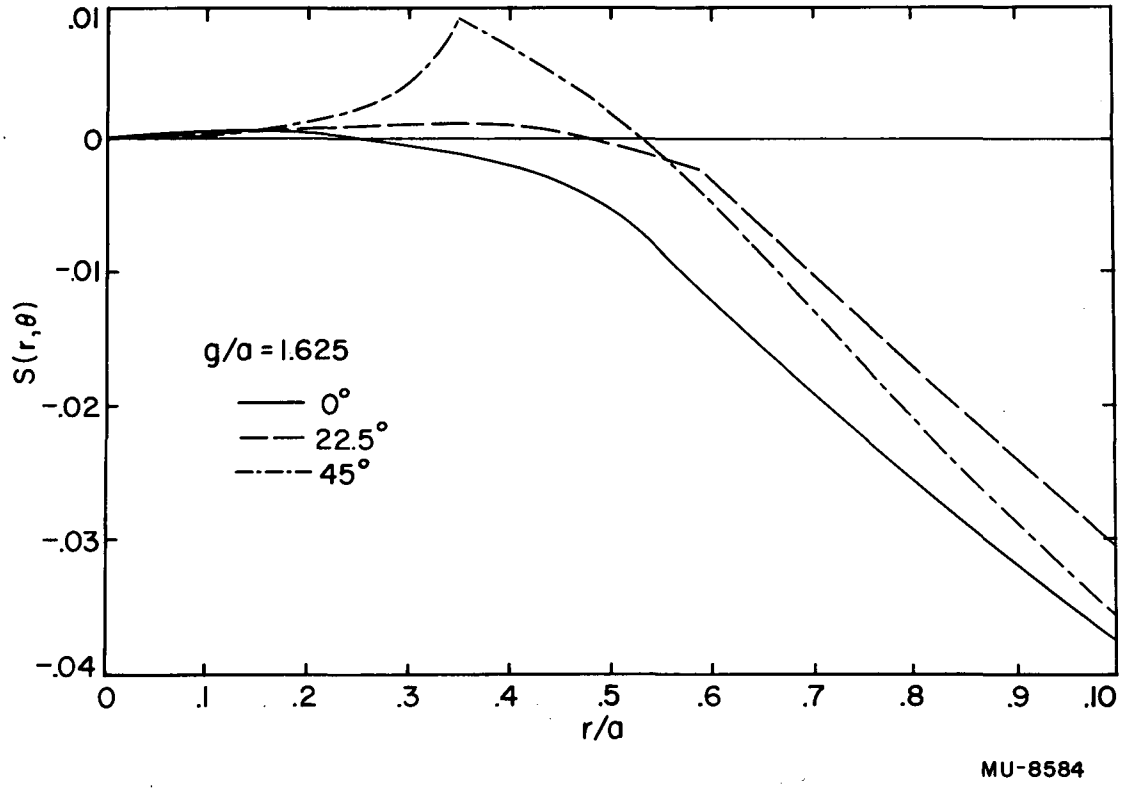

Fig. 6.

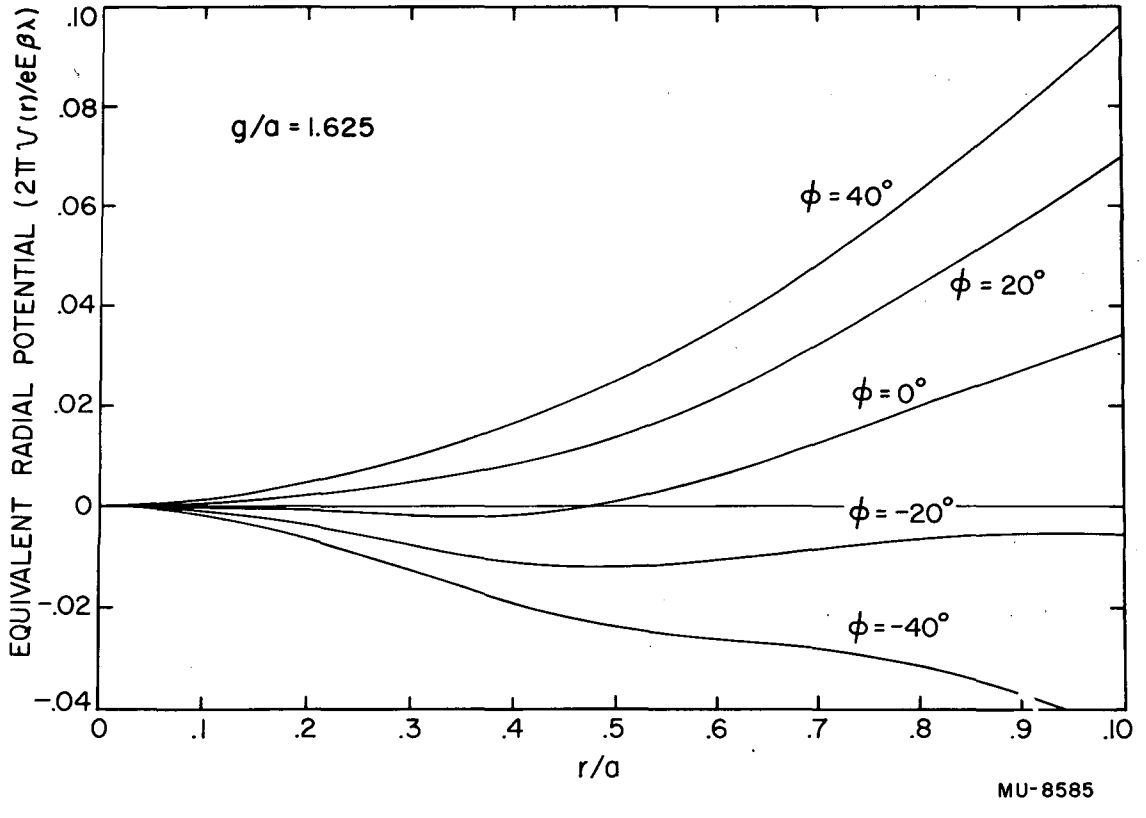
EQUIVALENT RADIAL POTENTIAL ($2\pi V(r)/eE\beta\lambda$)
.10
.08
.06
.04
.02
0
-.02
-.04
g/a = 1.625
ϕ = 40°
ϕ = 20°
ϕ = 0°
ϕ = -20°
ϕ = -40°
0
.1
.2
.3
.4
.5
.6
.7
.8
.9
.10
r/a
MU-8585

Fig. 7.

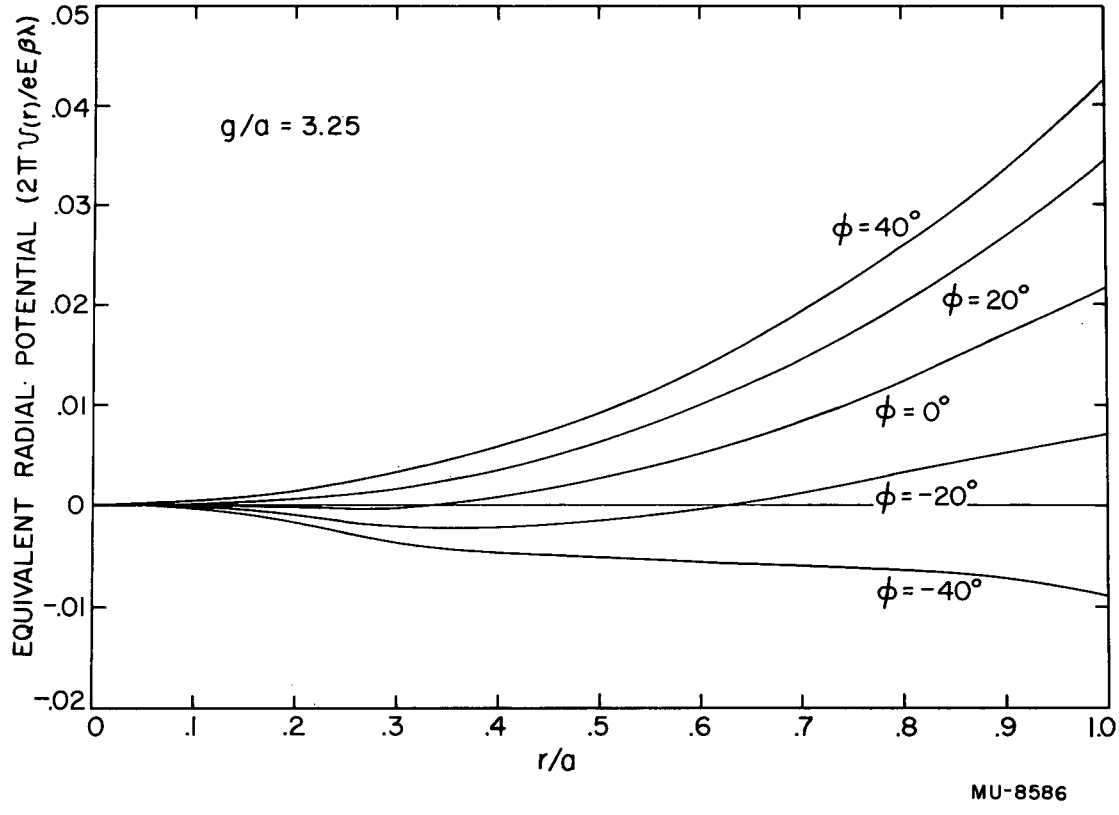
EQUIVALENT RADIAL POTENTIAL (2πV(r)/eEβλ)
.05
.04
.03
.02
.01
0
-.01
-.02
g/a = 3.25
φ = 40°
φ = 20°
φ = 0°
φ = -20°
φ = -40°
0
.1
.2
.3
.4
.5
.6
.7
.8
.9
1.0
r/a
MU-8586

Fig. 8.

$$V_o(r) = \frac{eE\beta\lambda}{2\pi}\left[\frac{\sqrt{2}\,\pi r^2}{(\beta\lambda)^2}(\cos\phi + \sin\phi)\right] . \qquad (35)$$

Phases as low as -45° will lead to stable motion, and the permissible kinetic energy of radial motion is 1.5 to 3 times as large as for the actual grids, depending on the phase. One therefore is faced with the fact that the angular and phase acceptance of a grid-focused machine is much smaller than might be expected.

The potential curves in Figs. 7 and 8 have only a qualitative value, for the phase and particle velocity vary with time. Numerical solutions to Eq. (32) were therefore obtained for various initial conditions.†† The actual orbits depend very sensitively on the initial conditions, but on the average the conclusions reached above are borne out; angular and phase acceptance of a grid machine are small.

These results suggest a measure that may be taken to improve beam transmission in an actual accelerator. Small synchronous phases should result in greater grid efficiency and therefore larger currents if a phase buncher or its equivalent is used. To permit operation at these phases, however, the uniformity of the accelerating field and the voltage regulation of various components of the accelerator will have to be maintained quite precisely.

Additional items of interest have arisen in the course of this investigation of grids:

(1) Measurements with grids containing only two of the four grid ribbons in Fig. 4 have been made for $g/a = 1.625$ and 3.25. They are about half as efficient as the four-element grids, that is, the phase limits for stable motion are approximately -10° and -15° respectively.

(2) An estimate of the azimuthal impulse received by the particle was made from the curves in Figs. 5 and 6. The effect of these impulses on the amplitude of radial motion does not appear to be serious for the heavy-ion machine, but may be important in longer accelerators.

---

††Orbits with perfect grids have been calculated by N. M. King, AERE-T/M-107, Harwell, Berks. (England) (1954) for a variety of initial conditions using a synchronous phase of -30°.

IV. SOLENOIDAL FOCUSING

The radial defocusing effect of the accelerating field can be counterbalanced in a straightforward way by introducing an axial magnetic field. This can be accomplished in the Alvarez-type accelerator by enclosing solenoidal magnets in the drift-tube shells, power being supplied through the drift-tube supports. The power required for adequate focusing is generally excessive, but the method has some unique features that make it attractive in special situations.

The equation describing the radial motion of an ion in the combined fields is†

$$\frac{d^2r}{dt^2} = -(\omega_H^2 - \omega_{RF}^2)r, \tag{36}$$

where

$$\omega_H^2 = \frac{1}{4}\left(\frac{eH}{mc}\right)^2, \quad \omega_{RF}^2 = \frac{-\pi eET \sin\phi}{m\beta\lambda} = -\nu^2\Delta, \tag{37}$$

assuming that the ion enters the accelerator with no angular momentum about the axis. If the magnetic field is confined mainly to the interior of the drift tubes, the motion is described sufficiently well by interpreting H as the root-mean-square value along the axis. Thus, if the magnetic field is sufficiently large, the radial position of the ion varies sinusoidally in time, with a frequency given by the net spring constant.

The attractive features of solenoidal focusing are apparent from a consideration of the orbit equation. The radial motion can be controlled independently of the accelerating field and without the restrictive stability conditions of a strong-focusing system. The net spring constant can be varied over a wide range of values as the ions progress through the accelerator, permitting a substantial control over the radial extent of the beam. Finally, the alignment problem is not as severe as in the case of strong-focusing lenses.

The required magnitudes of the magnetic fields depend upon the radial and angular spread of the entering beam and on the definition demanded of the

---

†See for example Zworykin et al. Electron Optics and the Electron Microscope, John Wiley and Sons, Inc., New York and London (1945), Chap. 15.

accelerated beam. A minimum level is determined by asking that the synchronous particle feel no net restoring force, that is, from Eqs. (36) and (37),

$$H_{min} = \left[\frac{4\pi mc^2}{e} \frac{ET|\sin \phi_s|}{\beta\lambda} \right]^{1/2} . \tag{38}$$

For a certain value of the magnetic field, such that the net radial frequency of the synchronous ion is half of the phase oscillation frequency, the time variation of ω_{RF}^2 for nonsynchronous particles may cause a growth in the amplitude of radial oscillation,† but in general the oscillations of ω_{RF}^2 about the synchronous value are unimportant. The magnetic field used should exceed H_{min} by an amount sufficient to offset the effects of fluctuations of rf gradient from gap to gap and pulse to pulse (perhaps 5 percent) and to accept the injected beam. The initial half-angle acceptance is

$$a_o = \frac{a(\omega_H^2 - \omega_{RF}^2)^{1/2}}{v_o} , \tag{39}$$

where a is the bore radius and v_o is the initial velocity. A parallel entering beam can, of course, fill the bore whatever the net restoring force, in marked contrast to the case of strong-focusing.

If the magnetic and electric forces change slowly along the accelerator, the output beam will have a diameter

$$D_f = D_o \frac{(\omega_H^2 - \omega_{RF}^2)_o^{1/4}}{(\omega_H^2 - \omega_{RF}^2)_f^{1/4}} \tag{40}$$

and a half angle

$$a_f = a_o \frac{v_o}{v_f} \frac{(\omega_H^2 - \omega_{RF}^2)_f^{1/4}}{(\omega_H^2 - \omega_{RF}^2)_o^{1/4}} , \tag{41}$$

where the subscripts denote initial and final values.

---

†A resonance effect similar to that discussed for strong-focusing.

As an example, consider the main section of the heavy-ion accelerator. At the entrance end, H_{min} ~10 kilogauss. An rms field of 11 kilogauss would be adequate to accept the beam anticipated from the preaccelerator. To maintain a beam of constant diameter, the magnetic field required diminishes toward the high-energy end to a value of 7 kilogauss. On the other hand, if the 11-kilogauss figure were maintained to the end, the high-energy beam would be decreased in diameter by a factor of 1.4.

The power required for solenoidal focusing in the heavy-ion machine has been estimated to exceed 5 Mw. This is an order of magnitude larger than the power needed using strong focusing magnets: ~70 kw for N = 2 and ~250 kw for N = 1.

APPENDIX

A. Phase Motion

A general discussion of the phase motion in a linear accelerator has been given by Panofsky[8], together with the definition of the transit time factor. That part of his development pertinent to the present work is reproduced here.

Longitudinal stability is achieved in a linear accelerator by having the ion cross the gap while the accelerating field is rising. An ion arriving too early at the following gap receives less than the usual velocity increment. In this way, oscillations take place about a synchronous phase and the longitudinal motion is stable.

The differential equation for the phase motion, where the impulsive action of the gaps is averaged over an rf cycle, is

$$\frac{d}{dt}\left(\beta^2 \frac{d\phi}{dt}\right) + \left(\frac{2\pi e E \beta T}{m\lambda}\right)(\cos\phi - \cos\phi_s) = 0 , \qquad (42)$$

where E is the average rf accelerating field and ϕ is the rf phase as the ion crosses the gap ($\phi = 0^\circ$ corresponds to maximum field). The transit time factor T represents the effect of the finite size of the gap g and bore a, and is the ratio of the energy gain in crossing a gap to the ideal value $e\Delta V \cos\phi$, i.e.

---

[8] W. K. H. Panofsky, "Linear Accelerator Beam Dynamics," University of California Radiation Laboratory Report No. UCRL-1216, February 1951.

$$T = \frac{\Delta W}{e\Delta V \cos\phi} \quad . \tag{43}$$

For a symmetric gap,

$$T \cong \frac{\int E_z \cos(\frac{2\pi z}{L})\, dz}{\int E_z\, dz} \cong \frac{\sin(\frac{\pi g}{L})}{(\frac{\pi g}{L})\, I_o(\frac{2\pi a}{L})} \tag{44}$$

for a particle traveling on the axis. Here $I_o(x) = J_o(ix)$ is the Bessel function of imaginary argument.

The phase motion described by Eq. (42) is similar to that in a synchrotron and corresponds to the motion of a pendulum with time-dependent loading and moment of inertia. For slowly varying parameters, one may obtain an approximate energy integral of Eq. (42) with a potential proportional to

$$\sin\phi - \phi\cos\phi_s \quad .$$

For small values of ϕ and ϕ_s one can show that the limits of stable phase are

$$2\phi_s < \phi < -\phi_s \quad , \tag{45}$$

where $\phi_s < 0$. The frequency of the phase oscillations for small phase amplitude is given by

$$\omega_\phi^{\,2} = \frac{-\pi eET \sin\phi_s}{m\beta\lambda} = -2\nu^2\Delta \quad , \tag{46}$$

where Δ defined in Eq. (7) is evaluated for $\phi = \phi_s$.

B. Radial Impulse

The radial impulse received by an ion in crossing a gap is given by

$$\Delta\dot{r} \cong \frac{e}{m\beta c}\int E_r \cos(\frac{2\pi z}{L} + \phi)\, dz \quad , \tag{47}$$

with

$$E_r \cong -\frac{1}{r}\int_o^r r\,\frac{\partial E_z}{\partial z}\, dr \quad . \tag{48}$$

Eq. (47) becomes, after integration by parts,

$$\frac{\Delta \dot{r}}{r} \cong - \frac{\pi e E}{m \beta c} \cdot \frac{2}{r^2} \int_0^r r dr \left[\frac{\int E_z \cos \left(\frac{2\pi z}{L} \right) + \phi) \, dz}{\int E_z \, dz} \right] . \qquad (49)$$

For a symmetric gap the quantity inside the brackets $\left[\; \right]$ may be expressed in terms of T in Eq. (44). For small r one then has

$$- \frac{\Delta \dot{r}}{r} \cong \Delta \cong \frac{\pi e E \lambda T \sin \phi}{mc^2 \beta} . \qquad (50)$$

ACKNOWLEDGMENT

The authors would like to thank Fred E. Holmquist, who performed the electrolytic tray measurements for the grids and contributed to the calculation of the stability regions in the quadrupole lens section. They also would like to acknowledge the assistance of Robert A. Weir and the differential analyzer group in the computation of orbits in a grid machine. Finally, one of the authors (RLG) is grateful to the Radiation Laboratory for its hospitality during the course of this work.

FIGURE LEGENDS

Fig. 1 Stability region and amplitude parameters for N = 1.

Fig. 2 Stability region and amplitude parameters for N = 2.

Fig. 3 Stability region and amplitude parameters for N = 3.

Fig. 4 Photograph of four-element grid used in the bevatron injector linac.

Fig. 5 $C(r, \theta)$ vs. r/a for the grid shown in Fig. 4 with g/a = 1.625, and $\theta = 0^\circ$, $22\ 1/2^\circ$, 45°.

Fig. 6 $S(r, \theta)$ vs. r/a for the grid shown in Fig. 4 with g/a = 1.625, and $\theta = 0^\circ$, $22\ 1/2^\circ$, 45°.

Fig. 7 Equivalent radial potential vs. r/a for various r-f phases with g/a = 1.625.

Fig. 8 Equivalent radial potential vs. r/a for various r-f phases with g/a = 3.25.

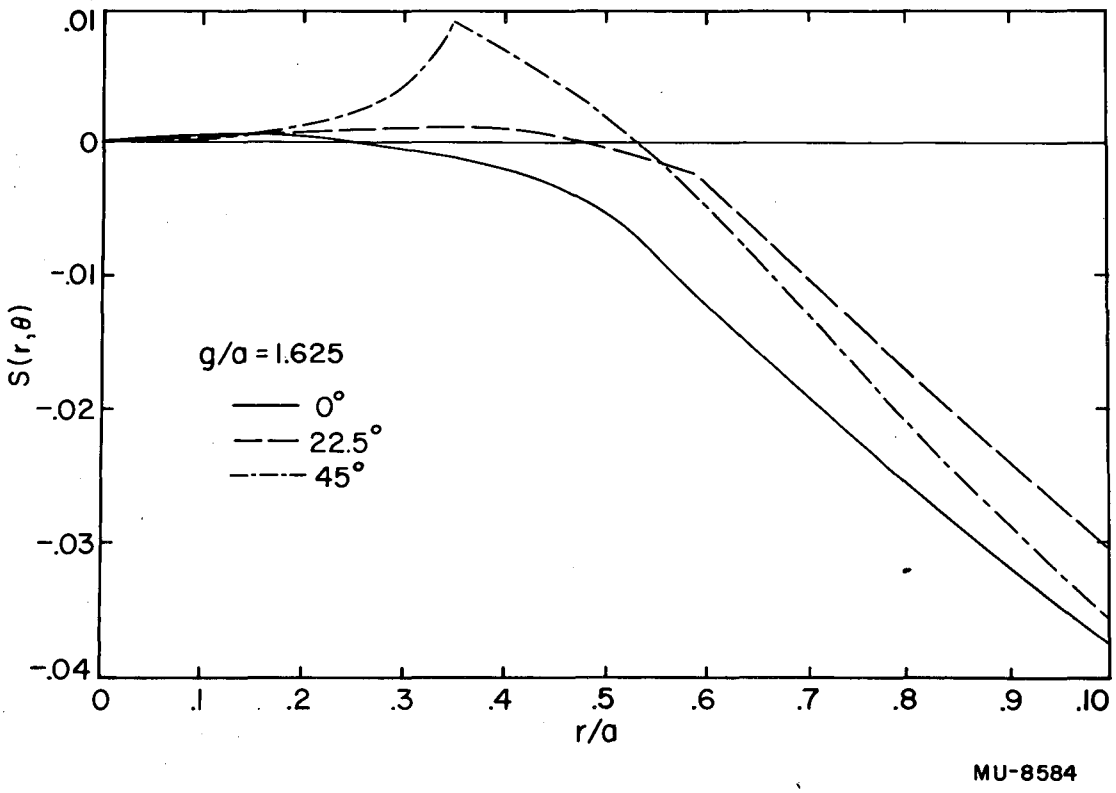

Fig. 6

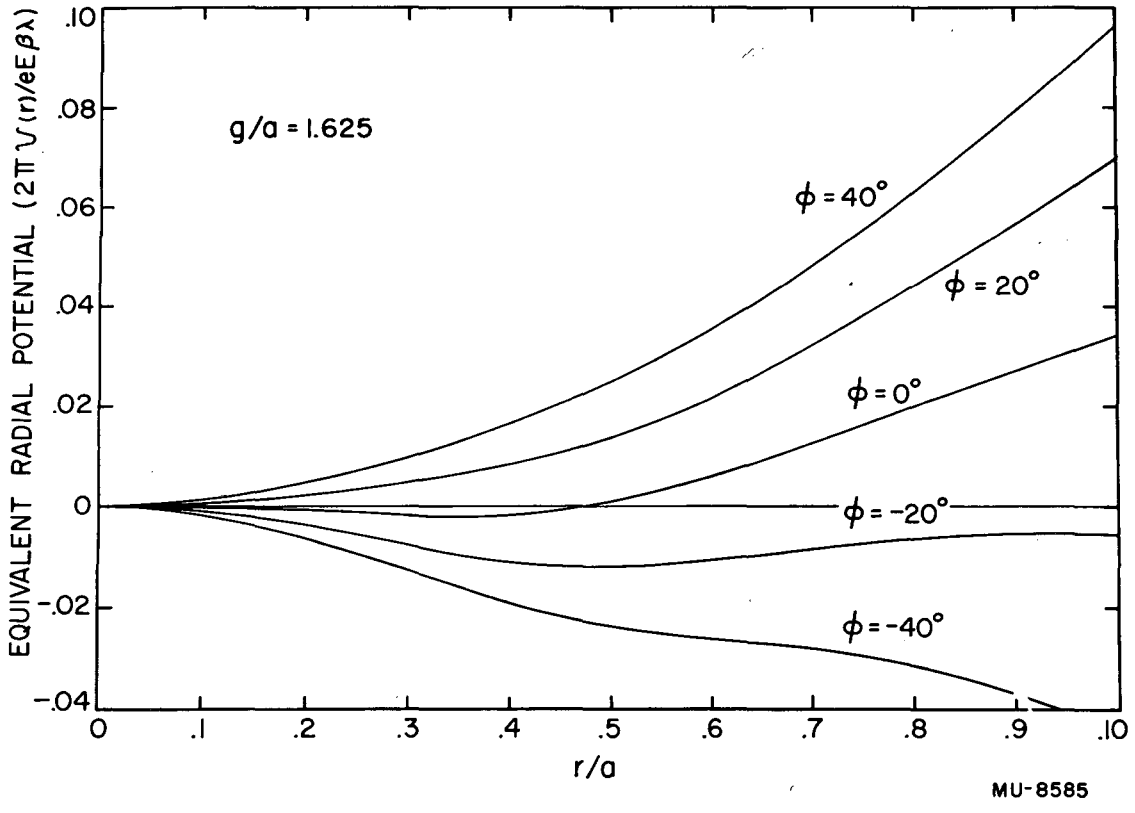
EQUIVALENT RADIAL POTENTIAL (2π V(r)/eEβλ)
.10
.08
.06
.04
.02
0
-.02
-.04
g/a = 1.625
φ = 40°
φ = 20°
φ = 0°
φ = -20°
φ = -40°
0
.1
.2
.3
.4
.5
.6
.7
.8
.9
.10
r/a
MU-8585

Fig. 7